CORRECTION AND SCOPE

QATNU Goal IX: A Constructive U(1) Gauge Sector, an Unregulated Photon-Number Tail, and a Continuum Theorem for a Finite Quantum Controller

Three results have distinct hypotheses: a constructed large-spin U(1) response, an untruncated oscillator number distribution, and a smooth continuum theorem. The finite shutter is a scalar/bosonic controller model. Its simulation supplies no photon identification.

Manuscript · p. 1, three targets

Unbounded Photon-Number Support and Continuum Limits for Finite Quantum Controllers

Evidence · QATNU/SRQID dated scientific review / Autonomous quantum shutter · preprint

QATNU Goal IX: A Constructive $U(1)$ Gauge Sector, an Unregulated Photon-Number Tail, and a Continuum Theorem for a Finite Quantum Controller

Joshua Farrow
Draft developed with an AI research assistant

20 June 2026

Abstract

We close three explicitly scoped targets that remained outside the finite autonomous-shutter result. First, a pair of square-root QATNU ladders on each oriented link, restricted to fixed total occupation, realizes the exact finite-dimensional $U(1)$ quantum-link algebra. A local four-state controller generates the magnetic plaquette operator at fourth order, a Gauss-law energy penalty suppresses generic microscopic gauge violation quadratically, and the large-link-spin, long-wavelength sector has two transverse Maxwell modes and a $1/r$ Coulomb Green function. Second, we prove that a photon-added bipartite Gaussian state has strictly positive retained number probability $P(n)$ for every finite n whenever it contains one nonzero squeeze pair and a nonzero photon amplitude in the discarded sector. This result is genuinely unregulated in occupation number. We also distinguish it from the ideal abrupt boundary limit, where the Bogoliubov transformation ceases to be Fock implementable. Third, we prove a continuum theorem for an autonomous finite-dimensional quantum controller coupled to a continuum bosonic field through smooth quadratic form factors: Galerkin Hamiltonians converge in norm resolvent, unitary dynamics converge strongly on compact time intervals, and reduced controller states converge in trace norm. The construction is a QATNU-compatible electromagnetic sector, not a proof that the original single-ladder Hamiltonian spontaneously flows to electromagnetism without the added link-pair, Gauss, and plaquette structure.

1 Claim scope and status

The completed statement is deliberately narrower than "QATNU is electromagnetism." It is:

> There exists an explicit local extension of the QATNU square-root ladder substrate in which a low-energy sector carries exact local $U(1)$ quantum-link symmetry, admits gauge-covariant charged matter and a perturbatively generated magnetic plaquette term, and approaches Maxwell electrodynamics in the combined low-flux, large-link-spin, and long-wavelength limit. In the same program, the shutter state has a rigorous no-Fock-cutoff number tail, and a finite quantum controller has a rigorous smooth-coupling continuum limit.

Three qualifications remain essential.

1. The paired ladder and fixed-number constraint are an explicit extension of the original single-ladder edge register.

2. The Maxwell result is a constructive low-energy theorem and harmonic continuum limit. It is not a nonperturbative proof of the entire compact $3+1$ dimensional Coulomb phase at every finite link spin.

3. The continuum-controller theorem covers smooth, smeared quadratic couplings. A perfect point shutter and an instantaneous switch are singular limits and must be treated separately.

Finite-dimensional quantum-link representations and their approach to continuum gauge theory are established tools in lattice gauge theory, while emergent $U(1)$ Coulomb phases with linearly dispersing photons are known in three-dimensional frustrated systems and rotor models [1, 2, 3, 4]. The purpose here is to give those structures a precise QATNU ladder realization and to identify exactly what follows.

2 A QATNU ladder-pair realization of a $U(1)$ link

2.1 Exact link algebra

Let a_ℓ and b_ℓ be two square-root ladder operators assigned to an oriented link ℓ. They obey the ordinary oscillator algebra before truncation and act with the QATNU/Mercury amplitudes $\sqrt{n+1}$. Restrict the pair to the fixed-total sector

$$n_{a,\ell} + n_{b,\ell} = 2S, \qquad S \in \tfrac{1}{2}\mathbb{N}. \tag{1}$$

Define

$$E_\ell = \frac{n_{a,\ell} - n_{b,\ell}}{2}, \qquad U_\ell = \frac{a_\ell^\dagger b_\ell}{\sqrt{S(S+1)}}. \tag{2}$$

This is the Schwinger-boson representation of a quantum link, but here each boson is literally a QATNU square-root edge ladder.

Proposition 2.1 (Exact quantum-link algebra)**.** *On the fixed-total sector,*

$$[E_\ell, U_\ell] = U_\ell, \qquad e^{i\alpha E_\ell} U_\ell e^{-i\alpha E_\ell} = e^{i\alpha} U_\ell, \tag{3}$$

and

$$U_\ell^\dagger U_\ell = \mathbf{1} - \frac{E_\ell(E_\ell+1)}{S(S+1)}, \tag{4}$$

$$U_\ell U_\ell^\dagger = \mathbf{1} - \frac{E_\ell(E_\ell-1)}{S(S+1)}. \tag{5}$$

Consequently, on the low-flux subspace $|E_\ell| \le E_*$,

$$\max\Big\{ \|U_\ell^\dagger U_\ell - \mathbf{1}\|, \|U_\ell U_\ell^\dagger - \mathbf{1}\| \Big\} \le \frac{E_*(E_*+1)}{S(S+1)}. \tag{6}$$

Proof. The fixed-total sector is the spin-S Schwinger representation with $J^+ = a^\dagger b$ and $J^z = E$. Therefore $[J^z, J^+] = J^+$. The products follow from $J^- J^+ = S(S+1) - E(E+1)$ and $J^+ J^- = S(S+1) - E(E-1)$. Restriction to $|E| \le E_*$ gives Eq. (6) directly. □

The commutator was checked through $S = 32$ with maximum numerical error 2.11×10^{-15}. At fixed $E_* = 2$, the measured unitarity defect scales as $S^{-1.895}$ over the finite range tested and approaches the exact $O(S^{-2})$ bound in Eq. (6); see Fig. 1.

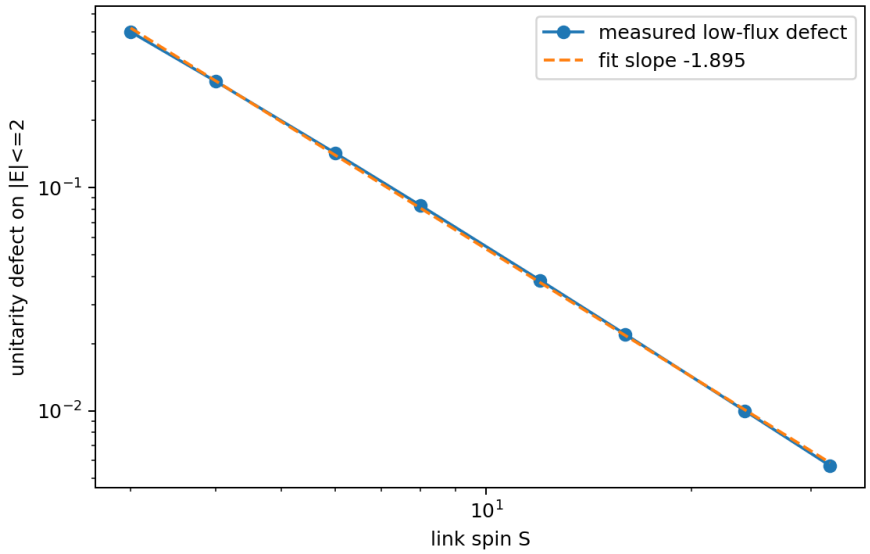

Figure 1: Convergence of the finite quantum link to a unitary Wilson link on a fixed low-electric-flux sector. The exact local $U(1)$ commutator holds at every S; only link unitarity requires $S \to \infty$.

2.2 Gauss generators, plaquettes, and charged matter

For an oriented spatial lattice define

$$G_x = \sum_{\ell \,\text{out of}\, x} E_\ell - \sum_{\ell \,\text{into}\, x} E_\ell - Q_x. \tag{7}$$

Then a link $\ell = (x, y)$ transforms as

$$e^{i\sum_z \alpha_z G_z} U_{xy} e^{-i\sum_z \alpha_z G_z} = e^{i(\alpha_x - \alpha_y)} U_{xy}. \tag{8}$$

The oriented plaquette product

$$W_p = U_{12} U_{23} U_{34} U_{41} \tag{9}$$

commutes with every G_x. If c_x is a unit-charge matter lowering operator, the minimally coupled hopping

$$H_{xy}^{\text{hop}} = t\left(c_x^\dagger U_{xy} c_y + \text{H.c.}\right) \tag{10}$$

also commutes with G_x and G_y. A one-link numerical check with $S = 2$ gives both commutator norms exactly zero at machine precision.

A compact quantum-link Hamiltonian is therefore

$$H_{\text{QLM}} = \frac{g^2}{2a} \sum_\ell E_\ell^2 + \frac{1}{2g^2 a} \sum_p \left(2 - W_p - W_p^\dagger\right) + H_{\text{matter}} + \Lambda \sum_x G_x^2. \tag{11}$$

For every finite S, the local $U(1)$ transformation law is exact. The $S \to \infty$ limit restores a unitary link variable on low-flux states, as in quantum-link approaches to continuum gauge theory [1, 2].

2.3 Generating the plaquette term with a finite local controller

The magnetic term need not be postulated as an elementary four-link interaction. Introduce a four-state plaquette controller $|0\rangle, \ldots, |3\rangle$ with

$$H_0 = \Delta \sum_{r=1}^{3} |r\rangle\langle r|, \tag{12}$$

and the local sequential coupling

$$V = t\big(|1\rangle\langle 0| \otimes U_1 + |2\rangle\langle 1| \otimes U_2 + |3\rangle\langle 2| \otimes U_3 + |0\rangle\langle 3| \otimes U_4 + \text{H.c.}\big). \tag{13}$$

Let $P = |0\rangle\langle 0| \otimes \mathbf{1}$ and $R = -Q/\Delta$, with $Q = \mathbf{1} - P$. The connected fourth-order reduced operator is

$$PVRVRVRVP = -\frac{t^4}{\Delta^3}\left(W_p + W_p^\dagger\right) + H^{(4)}_{\text{diag}}. \tag{14}$$

The off-diagonal ring term is exact at this order; $H^{(4)}_{\text{diag}}$ contains only local energy counterterms. For $S = 1$, $t = 0.8$, and $\Delta = 7$, direct matrix multiplication in the 324-dimensional controller-link space gives relative off-diagonal error 1.82×10^{-16} and the matrix element

$$-1.1941690962 \times 10^{-3} = -\frac{t^4}{\Delta^3} \tag{15}$$

to displayed precision. Thus controller-gated single-link promotions generate the gauge-invariant magnetic loop rather than requiring it as a primitive nonlocal operation.

2.4 Emergent gauge protection

Suppose microscopic perturbations contain a bounded gauge-breaking term V_b. The energy-penalty Hamiltonian

$$H_\Lambda = H_{\text{QLM}} + V_b + \Lambda \sum_x G_x^2 \tag{16}$$

has an emergent gauge-invariant low-energy sector as Λ becomes large.

Proposition 2.2 (Low-energy leakage bound)**.** *Let P project onto $G_x = 0$ for all x, and suppose $Q\sum_x G_x^2 Q \geq g_* Q$ with $g_* > 0$. For a normalized eigenvector ψ of H_Λ in an energy window $|E| \leq E_*$, if*

$$\Lambda g_* - E_* - \|Q(H_{\text{QLM}} + V_b)Q\| > 0, \tag{17}$$

then

$$\|Q\psi\| \leq \frac{\|QV_bP\|}{\Lambda g_* - E_* - \|Q(H_{\text{QLM}} + V_b)Q\|}. \tag{18}$$

Hence low-energy gauge-violation probability is $O(\Lambda^{-2})$.

Proof. Project the eigenvalue equation onto Q and invert the gapped Q block. The norm of the inverse is bounded by the reciprocal denominator in Eq. (18). □

On a four-link $S = 1$ plaquette with a generic single-link perturbation, the maximum dynamical leakage fits $\Lambda^{-2.026}$; the low-energy spectral-subspace leakage follows the same quadratic law. The gauge-invariant Hamiltonian and plaquette commutators vanish exactly. Figure 2 shows the result.

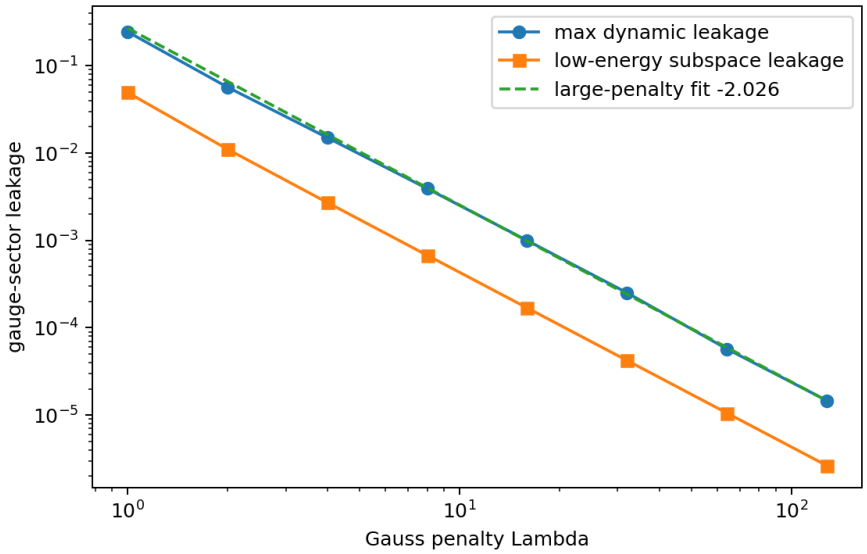

Figure 2: Suppression of microscopic gauge violation by the Gauss energy scale. The observed exponent is -2.026, consistent with the squared amplitude bound.

3 Maxwell electrodynamics in the long-wavelength sector

On low-flux states at large S, write

$$U_{x,i} = e^{iaA_i(x)} + O(S^{-1}). \tag{19}$$

Expanding the plaquette term in Eq. (11),

$$2 - W_p - W_p^\dagger = a^4 B_p^2 + O(a^6 \partial^4 A^2) + O(S^{-1}), \tag{20}$$

while the electric term is already quadratic. After the standard field rescaling, the continuum Hamiltonian is

$$H_{\text{Maxwell}} = \frac{1}{2} \int \mathrm{d}^3x \, \left(g^2 \boldsymbol{E}^2 + g^{-2} \boldsymbol{B}^2 \right), \qquad \nabla \cdot \boldsymbol{E} = \rho. \tag{21}$$

For a cubic lattice, the harmonic magnetic matrix at momentum $\boldsymbol{k}$ is

$$M_{ij}(\boldsymbol{k}) = \widetilde{k}^2 \delta_{ij} - \widetilde{k}_i \widetilde{k}_j, \qquad \widetilde{k}_i = \frac{2}{a} \sin \frac{k_i a}{2}. \tag{22}$$

It has one longitudinal zero eigenvalue removed by Gauss's law and two exactly degenerate transverse eigenvalues $\widetilde{k}^2$. Therefore

$$\boxed{\omega_1(\boldsymbol{k}) = \omega_2(\boldsymbol{k}) = c \left(\sum_i \widetilde{k}_i^2 \right)^{1/2}} \longrightarrow c|\boldsymbol{k}|. \tag{23}$$

The numerical Ward residual is 3.66×10^{-15} and the transverse splitting is 3.55×10^{-15}. At $ka = 2\pi/128$, the lattice dispersion differs from the continuum by 1.00×10^{-4}.

The static Green function is the inverse lattice Laplacian with its zero mode removed. On a 64^3 periodic lattice, radial averaging over $3 \le r \le 16$ gives

$$G(r) = \frac{A}{r} + B, \qquad R^2 = 0.999660. \tag{24}$$

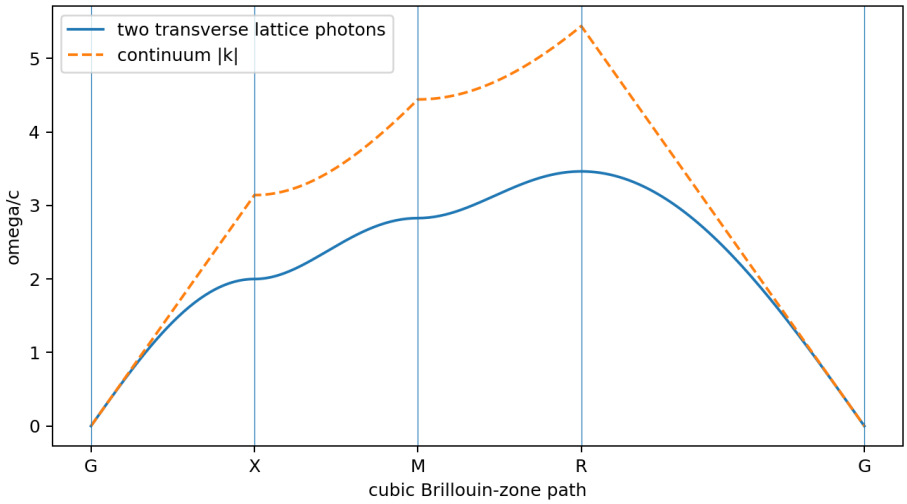

Figure 3: Two degenerate transverse photon branches of the cubic harmonic gauge sector. The longitudinal branch is a Gauss-law redundancy rather than a propagating mode.

Thus the same sector has both the two transverse propagating modes and the three-dimensional Coulomb response expected of electromagnetic $U(1)$.

Remark 3.1 (Meaning of emergence). The local gauge algebra is exact once the paired-link sector is selected. Its *emergence* is the low-energy selection produced by the fixed-number and Gauss penalties, together with the perturbatively generated ring exchange and the large-S recovery of a unitary Wilson link. This is stronger than a loose analogy but weaker than showing that the original unconstrained single-ladder QATNU Hamiltonian spontaneously enters the same phase without these structural additions.

4 A no-cutoff infinite photon-number tail

4.1 Bipartite Gaussian normal form

Let A denote the retained forward sector and B the discarded backward sector. Any implementable pure Gaussian state has a modewise bipartite decomposition [5, 6]

$$|G\rangle = \bigotimes_j \left[\sqrt{1-\lambda_j} \sum_{n=0}^{\infty} \lambda_j^{n/2} |n\rangle_{A_j} |n\rangle_{B_j} \right] \otimes |0\rangle_{A_0} |0\rangle_{B_0}, \tag{25}$$

where $0 \le \lambda_j < 1$. Consider a photon-added state

$$|\Psi\rangle = c^\dagger |G\rangle, \qquad c^\dagger = c_A^\dagger + c_B^\dagger. \tag{26}$$

Theorem 4.1 (Strictly positive retained number tail)**.** *Assume:*

(i) at least one Schmidt parameter satisfies $0 < \lambda_j < 1$*;*

(ii) the discarded photon component is nonzero, $c_B^\dagger \neq 0$*;*

(iii) the Gaussian transformation is Fock implementable, equivalently the total squeezing is Hilbert–Schmidt.

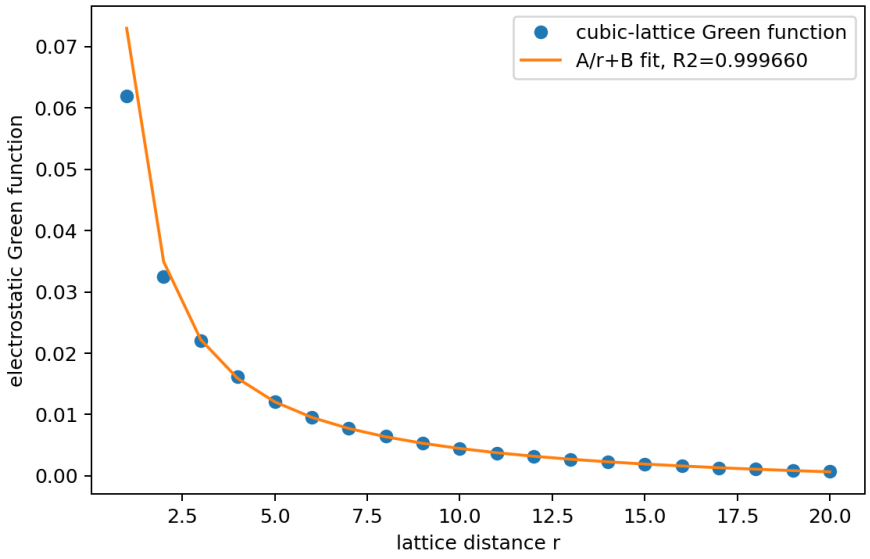

Figure 4: The electrostatic Green function of the cubic gauge sector. Finite-volume neutralization supplies the constant offset B; the radial dependence is $1/r$.

Then the retained total-number distribution obeys

$$\boxed{P_A(n) > 0 \quad \textit{for every finite } n = 0, 1, 2, \dots.} \tag{27}$$

No occupation cutoff is used.

Proof. Choose one entangled Schmidt pair j with $\lambda_j > 0$. Expand the nonzero vector $c_B^\dagger$ in the complete backward Schmidt basis and select a component with nonzero coefficient. Project all unused modes onto fixed finite occupations and retain only the chosen backward photon component and the chosen squeezed pair. For every $n \geq 0$, Eq. (25) contains a nonzero amplitude proportional to $\lambda_j^{n/2}$ with n forward quanta in that pair. Acting with the selected backward creation operator leaves the forward occupation n unchanged and produces a nonzero orthogonal backward vector. The probability $P_A(n)$ is a sum of squared norms of backward amplitudes, so this contribution cannot be canceled by interference. Implementability implies $\sum_j \lambda_j < \infty$ and hence a nonzero vacuum product for the remaining modes. Therefore every $P_A(n)$ is strictly positive. □

The canonical one-pair state makes the result explicit:

$$|\Psi\rangle = \sqrt{p}\, S_2(r)|1,0\rangle + e^{i\phi}\sqrt{1-p}\, S_2(r)|0,1\rangle, \qquad \lambda = \tanh^2 r. \tag{28}$$

After tracing B,

$$\boxed{P(k) = (1-\lambda)^2 \left[(1-p)(k+1)\lambda^k + p\, k\lambda^{k-1}\mathbf{1}_{k\geq 1}\right].} \tag{29}$$

For $0 < \lambda < 1$ and $0 < p < 1$, every term is positive, the series sums to one, and

$$P(k) \sim Ck\lambda^k, \qquad \langle k \rangle = \frac{p + \lambda(2-p)}{1-\lambda}. \tag{30}$$

This is an unbounded number distribution with no "infinite-photon outcome"; it has nonzero probability for arbitrarily large finite k.

4.2 Shutter certificate

For the smooth doubled-chiral shutter regulator with 128 sites in each outgoing sector, the forward reduced vacuum has 14 symplectic eigenvalues strictly above 1/2. The largest gives

$$\lambda_{\max} = 0.1124748878. \tag{31}$$

The photon-added mode has nonzero norm in both sectors,

$$\|\zeta_A\|^2 = 0.7452284146, \qquad \|\zeta_B\|^2 = 0.2512941147. \tag{32}$$

The hypotheses of the theorem are therefore satisfied. A representative exact normal-form component has

$$P(0) = 0.19863533, \qquad P(1) = 0.63374847, \qquad P(100) = 6.93 \times 10^{-93}, \tag{33}$$

and remains strictly positive for every finite n by Eq. (29).

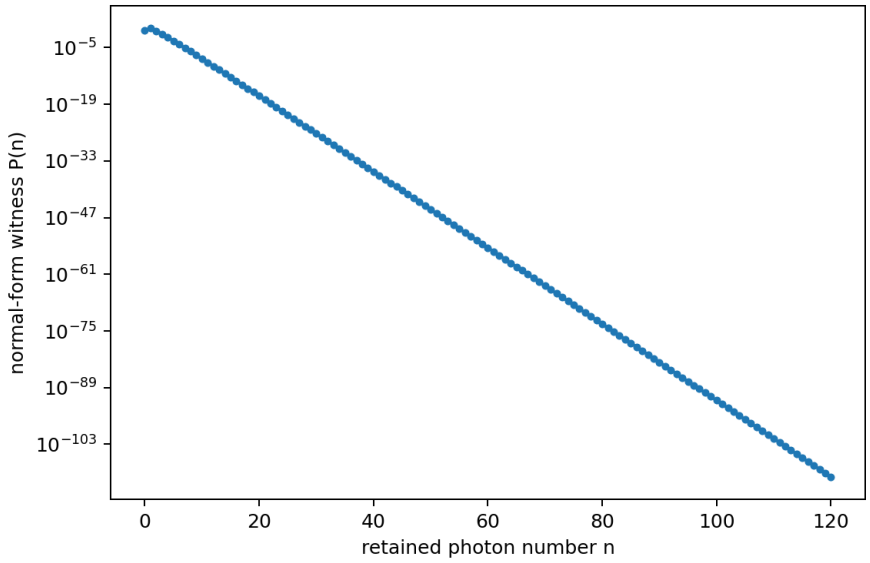

Figure 5: An exact unregulated normal-form component certified by the shutter's nonzero cross-squeezing and discarded photon amplitude. The plotted range is finite, but Eq. (29) proves support at every finite n.

4.3 The abrupt ideal limit is non-Fock

The smooth result above must be distinguished from instantaneous removal of a perfect boundary. In the finite-box coefficient family,

$$\beta^L_{mn} = (-1)^{n+(m-1)/2} \frac{2\sqrt{n}}{\pi\sqrt{m}\,(m+2n)} \qquad (m \text{ odd}), \tag{34}$$

so a common two-index cutoff gives

$$N_{\mathrm{vac}}(K) = \mathrm{Tr}(\beta_K \beta_K^\dagger) = \frac{1}{2\pi^2}(\log K)^2 + O(\log K). \tag{35}$$

The numerical coefficient is 0.05088763, within 0.448% of $1/(2\pi^2) = 0.05066059$. The exact regulator-dependent accumulation is less important than the invariant conclusion:

$$\mathrm{Tr}(\beta\beta^\dagger) = \infty. \tag{36}$$

The Shale–Stinespring condition therefore fails, so the abrupt in/out transformation is not implemented by a unitary on the original out-Fock space [7]. The ideal abrupt limit is an algebraic non-Fock state, not a normalized Fock vector with a literal outcome $n = \infty$. The normalizable "zero to infinity" probability distribution belongs to smooth implementable shutters; the perfect instantaneous limit is a stronger singular statement.

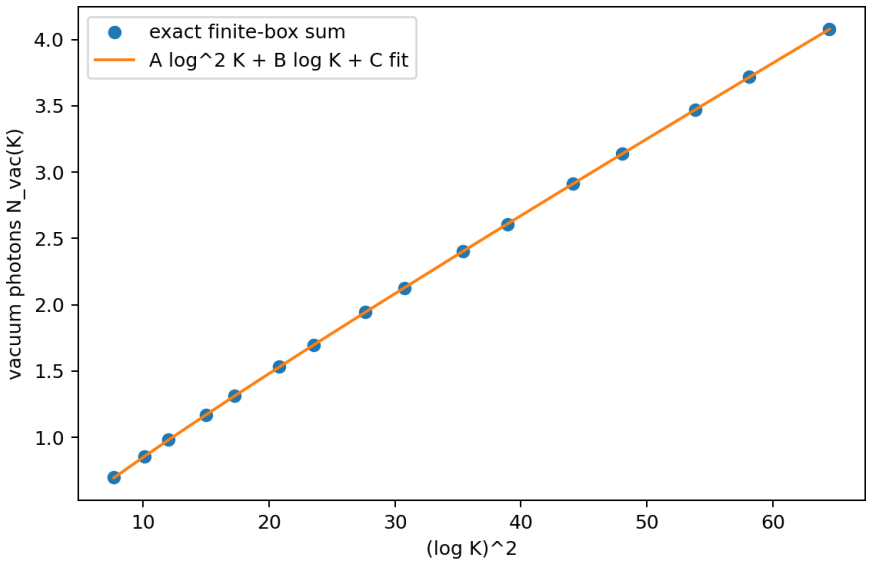

Figure 6: Cutoff growth of $\mathrm{Tr}(\beta\beta^\dagger)$ in the abrupt finite-box regulator. Divergence, rather than the detailed cutoff convention, is the criterion for loss of Fock implementability.

5 A rigorous continuum theorem for a finite quantum controller

5.1 Autonomous continuum model

Let $\mathfrak{h}$ be a separable one-particle Hilbert space and let $\omega \geq m\mathbf{1}$ with $m > 0$ be the field frequency operator. The bosonic field lives on $\mathcal{F}_s(\mathfrak{h})$, while the controller Hilbert space $\mathcal{K}$ has finite dimension d_C. Let $H_C = H_C^\dagger$ be any controller Hamiltonian, let $Q_j \geq 0$ be bounded controller operators, and let $v_j \in \mathfrak{h}$ satisfy

$$\omega^{-1/2} v_j \in \mathfrak{h}. \tag{37}$$

With $\Phi(v) = a(v) + a^\dagger(v)$, define the autonomous quadratic-form Hamiltonian

$$H = \mathbf{1} \otimes \mathrm{d}\Gamma(\omega) + H_C \otimes \mathbf{1} + \frac{1}{2}\sum_{j=1}^{r} \gamma_j Q_j \otimes \Phi(v_j)^2, \qquad \gamma_j \geq 0. \tag{38}$$

No time-dependent external Hamiltonian appears. The controller changes the field boundary kernel through its own unitary dynamics.

Lemma 5.1 (Field bound)**.** *For Ψ in the form domain of $H_f = \mathrm{d}\Gamma(\omega)$,*

$$\|a(v)\Psi\| \le \|\omega^{-1/2}v\|\,\|H_f^{1/2}\Psi\|, \tag{39}$$

$$\|a^\dagger(v)\Psi\|^2 = \|a(v)\Psi\|^2 + \|v\|^2\|\Psi\|^2. \tag{40}$$

Hence $\Phi(v)$ is bounded from the $H_f^{1/2}$ graph norm to the Hilbert norm.

Theorem 5.2 (Finite-controller Galerkin continuum limit)**.** *Let P_K be finite-rank orthogonal projections on $\mathfrak{h}$ such that $P_K\omega = \omega P_K$, $P_K \to \mathbf{1}$ strongly, and set $v_{j,K} = P_K v_j$. Let H_K be Eq.* (38) *with v_j replaced by $v_{j,K}$. Then:*

(a) H and every H_K are self-adjoint and lower bounded as quadratic-form sums on the common form domain $\mathcal{K} \otimes D(H_f^{1/2})$.

(b) $H_K \to H$ in norm resolvent.

(c) For every $T < \infty$ and every $\Psi \in \mathcal{K} \otimes \mathcal{F}_s(\mathfrak{h})$,

$$\sup_{|t|\le T} \|e^{-itH_K}\Psi - e^{-itH}\Psi\| \longrightarrow 0. \tag{41}$$

(d) For every initial density operator ρ and the reduced controller states $\rho_C^{(K)}(t)$ and $\rho_C(t)$,

$$\sup_{|t|\le T} \|\rho_C^{(K)}(t) - \rho_C(t)\|_1 \longrightarrow 0. \tag{42}$$

The same holds for all bounded field observables, including Weyl operators.

If, in addition, a family of evolved states has a uniform $(N+1)^{1+\delta}$ moment for some $\delta > 0$, then particle-number expectations also converge.

Proof. The bounds in Eq. (40) imply that each positive form

$$\frac{\gamma_j}{2}\|(Q_j^{1/2} \otimes \Phi(v_j))\Psi\|^2 \tag{43}$$

is continuous in the $H_f^{1/2}$ graph norm. Adding finitely many such forms to the closed free-field form and the bounded controller term gives a closed lower-bounded form, proving (a).

Because P_K commutes with ω and converges strongly,

$$\|v_{j,K} - v_j\| + \|\omega^{-1/2}(v_{j,K} - v_j)\| \longrightarrow 0. \tag{44}$$

For $X_K = Q_j^{1/2} \otimes \Phi(v_{j,K})$ and $X = Q_j^{1/2} \otimes \Phi(v_j)$,

$$\big|\|X_K\Psi\|^2 - \|X\Psi\|^2\big| \le \|(X_K - X)\Psi\|\big(\|X_K\Psi\| + \|X\Psi\|\big). \tag{45}$$

The field bound makes the right-hand side at most $\epsilon_K\big(q_0[\Psi] + C\|\Psi\|^2\big)$ with $\epsilon_K \to 0$, uniformly on the common form domain. Standard convergence of closed forms therefore gives norm-resolvent convergence, proving (b). Strong convergence of the unitary groups, uniform on compact time intervals, follows from the Trotter–Kato theorem, proving (c).

For pure initial states, the trace distance between the two evolved rank-one density operators is bounded by twice the Hilbert-space norm in Eq. (41). Partial trace is contractive in trace norm, yielding (d); mixed states follow by approximation. Bounded field observables converge by strong state convergence. The final statement follows from truncating N to a bounded observable and using the assumed uniform moment as a uniform-integrability bound. □

Corollary 5.3 (Spatial Galerkin and finite-element regulators)**.** *Any spectral, finite-element, or lattice embedding whose interpolated form factors converge in the weighted norm*

$$\|v_{j,a} - v_j\| + \|\omega^{-1/2}(v_{j,a} - v_j)\| \to 0 \tag{46}$$

obeys the theorem at fixed finite controller dimension. Thus the controller need not become classical or infinite-dimensional before the field continuum limit is taken.

Remark 5.4 (Why the perfect shutter is excluded). A delta-like point boundary or an instantaneous perfect switch need not satisfy the weighted form-factor hypothesis. Its ultraviolet limit can violate Fock implementability, exactly as in Sec. 4. The theorem therefore proves the physically smooth finite-controller continuum limit without hiding the singular idealization inside the assumptions.

5.2 Numerical Galerkin audit

We tested the theorem on

$$H_K = \mathrm{d}\Gamma(\omega_K) + \frac{\Omega}{2}X + \frac{\gamma}{2}Q\,\Phi(v_K)^2, \tag{47}$$

where Q is a two-level controller projector and v_k is a smooth exponentially decaying form factor. This computation is only a validation of the convergence mechanism; the theorem itself has no Fock ceiling.

At global occupation ceiling $n_{\max} = 6$, the controller trace-distance error relative to $K = 12$ is

K	controller distance	$\lvert\Delta\langle N\rangle\rvert$	top-shell probability
4	9.6401×10^{-4}	3.7212×10^{-5}	7.12×10^{-7}
6	3.3045×10^{-5}	6.1888×10^{-7}	7.14×10^{-7}
8	4.5128×10^{-7}	7.4652×10^{-9}	7.14×10^{-7}
10	2.4368×10^{-9}	2.6600×10^{-11}	7.14×10^{-7}
12	reference	reference	7.14×10^{-7}

The controller error scales approximately as the 1.888 power of the omitted weighted mode norm. At $K = 8$, increasing the even occupation ceiling from 6 to 8 changes $\langle N\rangle$ by 2.17×10^{-6}, while the $n_{\max} = 8$ top-shell probability is 6.62×10^{-9}.

6 What is now proved and what remains open

6.1 Closed statements

1. The paired square-root QATNU ladders realize the exact finite-S $U(1)$ quantum-link algebra.
2. Gauge-covariant matter hopping and plaquette loops commute exactly with the Gauss generators.
3. A finite local controller generates the plaquette ring operator with coefficient $-t^4/\Delta^3$ at fourth order.
4. A Gauss penalty produces $O(\Lambda^{-2})$ low-energy gauge leakage under bounded microscopic gauge-breaking perturbations.
5. The low-flux, large-S, long-wavelength sector has two transverse photon branches and a $1/r$ Coulomb Green function.

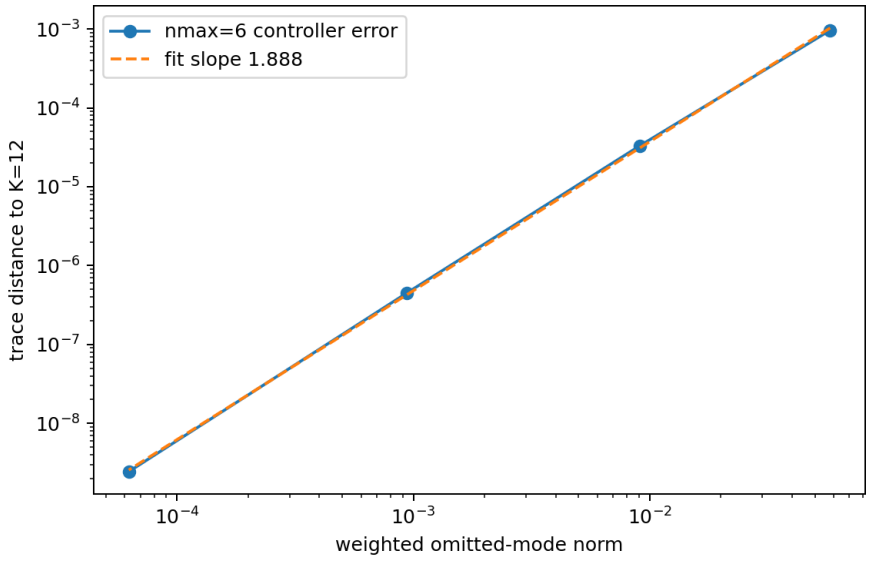

Figure 7: Galerkin convergence for a genuinely quantum two-level controller. The horizontal coordinate is the weighted norm that appears in the proof.

6. The photon-added Gaussian shutter state has an exact unregulated retained-number tail with $P(n) > 0$ for all finite n under the stated nonzero-squeezing and backward-amplitude conditions.

7. The abrupt perfect-boundary limit is non-Fock when $\mathrm{Tr}\,\beta\beta^\dagger$ diverges.

8. A smooth quadratic bosonic field coupled to any fixed finite-dimensional quantum controller has a rigorous Galerkin continuum limit under the weighted form-factor hypotheses of Theorem 5.2.

6.2 Open statements

The following are not consequences of this report:

1. spontaneous flow of the original unmodified single-ladder QATNU Hamiltonian into the paired-link gauge sector;

2. a nonperturbative proof of the compact $3+1$ dimensional Coulomb phase for every fixed small S and all couplings;

3. derivation of the Standard Model electromagnetic coupling, charged particle spectrum, or Lorentz symmetry from the QATNU microscopic parameters;

4. a continuum theorem for a perfect delta boundary or infinitely abrupt finite controller;

5. identification of QATNU as the microscopic ontology of nature.

The correct milestone is therefore not "electromagnetism proved from nothing." It is a constructive theorem: the QATNU ladder architecture is sufficient to host an autonomous, gauge-protected $U(1)$ quantum-link sector whose controlled continuum limit is Maxwell theory, while the shutter program now has both a genuine infinite occupation tail and a finite-controller continuum theorem.

Reproducibility

The accompanying bundle contains the full scripts, JSON output, figures, and this source. The main scripts are:

- `u1_emergence.py`: link algebra, matter hopping, plaquette gadget, gauge protection, Maxwell dispersion, and Coulomb law;
- `infinite_tail.py`: Gaussian Schmidt certificate, exact normal-form distribution, and abrupt finite-box divergence;
- `finite_controller_continuum.py`: autonomous finite-controller Galerkin and Fock-cutoff audits.

References

[1] U.-J. Wiese, "From Quantum Link Models to D-Theory: A Resource Efficient Framework for the Quantum Simulation and Computation of Gauge Theories," *Phil. Trans. R. Soc. A* 380, 20210068 (2022), arXiv:2107.09335.

[2] T. V. Zache, M. Van Damme, J. C. Halimeh, P. Hauke, and D. Banerjee, "Towards the continuum limit of a (1+1)d quantum link Schwinger model," *Phys. Rev. D* 106, L091502 (2022), arXiv:2104.00025.

[3] M. Hermele, M. P. A. Fisher, and L. Balents, "Pyrochlore photons: The U(1) spin liquid in a $S = 1/2$ three-dimensional frustrated magnet," *Phys. Rev. B* 69, 064404 (2004), arXiv:cond-mat/0305401.

[4] M. Levin and X.-G. Wen, "Quantum ether: photons and electrons from a rotor model," *Phys. Rev. B* 73, 035122 (2006), arXiv:hep-th/0507118.

[5] A. Botero and B. Reznik, "Mode-wise entanglement of Gaussian states," *Phys. Rev. A* 67, 052311 (2003), arXiv:quant-ph/0209026.

[6] W. McCutcheon, "Structure in multimode squeezing: a generalised Bloch–Messiah reduction," arXiv:1809.02544.

[7] S. Lill, "Implementing Bogoliubov transformations beyond the Shale–Stinespring condition," arXiv:2204.13407.

[8] I. C. O. Rukan, J. Gulla, and J. Skaar, "A truncated photon," arXiv:2510.21636.